Worldwide Mission Planning Tool for Tactical Laser Systems

Steven T. Fiorino[*] , Richard J. Bartell[†] , Matthew J. Krizo[‡] , Glen P. Perram[§] , Daniel J. Fedyk[¶] ,
Kenneth P. Moore[¶], Thomas R. Harris[¶], and Salvatore J. Cusumano[#]
Air Force Institute of Technology, Ohio 45433-7765

The directed energy modeling and simulation community can make important direct contributions to the joint warfighting community by providing the capability to estimate expected performance of high energy laser systems on a worldwide basis over both land and ocean regions accounting for variability in system performance arising from spatial, spectral and temporal variations in operating conditions. Key recently introduced features of the Air Force Institute of Technology Center for Directed Energy's high energy laser end-to-end operational simulation parametric one-on-one engagement level model allow it to meet modeling and simulation needs and function as a near term mission planning tool. These features include the capability to derive vertical profiles of atmospheric effects based probabilistic climatology, historical weather reanalysis grids, or real-time forecast models available on-line. Each atmospheric gas or particulate is evaluated based on its wavelength-dependent forward and off-axis scattering characteristics and absorption effects on electromagnetic energy delivered at any wavelength from 0.4 μm to 8.6 m. High energy laser end-to-end operational simulation can produce profiles, including correlated optical turbulence profiles in percentile format, from probabilistic climatology for over 400 land sites worldwide for all times of day and for a 1° × 1° grid over all ocean locations. In addition, probability of cloud free line of sight for hundreds of land sites worldwide is available in the model. Target surface orientation is defined in three-dimensional space, supporting accurate assessment of the effectiveness of a particular engagement geometry. Effects of thin layers of fog, several types of rain and several types of water droplet and ice clouds can also be considered. In the current study, performance predictions at several wavelengths for a number of geographically diverse land and sea locations are made using numerical weather reanalysis data and are compared with results derived from probabilistic climatology. Use of web-based

---

* Assistant Professor, Engineering Physics Department, Air Force Institute of Technology, 2950 Hobson Way, Wright-Patterson AFB, OH 45433-7765.

† Research Physicist, Center for Directed Energy, Air Force Institute of Technology, 2950 Hobson Way, Wright-Patterson AFB, OH 45433-7765.

‡ Research Engineer, Center for Directed Energy, Air Force Institute of Technology, 2950 Hobson Way, Wright-Patterson AFB, OH 45433-7765.

§ Professor, Engineering Physics Department, Air Force Institute of Technology, 2950 Hobson Way, Wright-Patterson AFB, OH 45433-7765.

¶ Research Assistant, Engineering Physics Department, Air Force Institute of Technology, 2950 Hobson Way, Wright-Patterson AFB, OH 45433-7765.

Center Director, Center for Directed Energy, Air Force Institute of Technology, 2950 Hobson Way, Wright-Patterson AFB, OH 45433-7765.

numerical weather data constitutes a step toward the development of a true directed energy mission planning tool. Complex interactions between the effects of meteorological parameters as a function of location, specific time of day, and season on predicted laser system performance have been demonstrated. Use of gridded numerical weather reanalysis data reveals operationally relevant changes in predicted system performance over fairly localized areas, indicating that in many cases conditions exist which might be exploited for operational advantage in employment of directed energy weapons if correctly forecasted and analyzed.

I.   Introduction

THE directed energy modeling and simulation (M&S) community can make important direct contributions to the joint warfighting community by establishing clear and fully integrated future program requirements. These requirements are best determined via analysis of the expected variability/uncertainty in system performance arising from spatial, spectral, and temporal variations in operating conditions. In the study described herein, the high energy laser end-to-end operational simulation (HELEEOS) M&S tool is used to evaluate the expected performance of laser systems operating at operationally relevant power levels at two wavelengths, 1.0624 μm and 1.31525 μm, for a number of widely dispersed land and maritime northern hemisphere locations.

Typically, researchers and systems developers have used HELEEOS with atmospheric effects generated by an internal probabilistic climatology to produce performance assessments with variability driven by the environmental effects. For this research, HELEEOS performance assessments are also produced using gridded National Centers for Environmental Prediction (NCEP) and National Center for Atmospheric Research (NCAR) weather reanalysis [1] data obtained from the open internet. This allows a direct comparison between effects caused by seasonal (winter and summer) probabilistic climatology and effects due to weather on specific dates (15 January 2007 and 15 July 2007) and times. This is notable because weather reanalysis grids are available in the same format from the same internet sites as gridded numerical weather prediction data. Demonstrating the capability to ingest and process reanalysis data demonstrates a similar capability to utilize real-time weather forecast data—and thus displaying the near-term mission planning capability of a potential decision aid such as HELEEOS.

A stressing tactical engagement geometry is used to emphasize the impact of climate effects. Results for this low altitude oblique slant range scenario indicate thermal blooming effects are significant for both wavelengths and there is considerable geographic variation in predicted system performance for 1.0624 μm. The next largest causes of variability/uncertainty are, respectively, aerosol extinction and optical turbulence effects, which can mitigate the effects of thermal blooming to a limited extent.

A. Description of the HELEEOS Model

HELEEOS supports dynamic engagements in which the platform, target and up to two optical relays can move vertically and horizontally on any heading in a true three-dimensional engagement. Engagement geometry is defined in HELEEOS by user specification of slant ranges, altitudes, headings, horizontal and vertical velocities, and horizontal and vertical accelerations. HELEEOS was developed by the Air Force Institute of Technology Center for Directed Energy under the sponsorship of the High Energy Laser Joint Technology Office, and its basic features have been previously described [2].

The HELEEOS model enables the evaluation of uncertainty in low-altitude laser propagation due to most major atmospheric effects. Atmospheric parameters investigated include profiles of temperature, pressure, water vapor content, optical turbulence, and atmospheric particulates as they relate to layer extinction coefficient magnitude. Worldwide seasonal, diurnal, and geographical spatial–temporal variability in these parameters is organized into probability density function (PDF) databases using a variety of resources to include the Extreme and Percentile Environmental Reference Tables (ExPERT) [3], the *Master Database for Optical Turbulence Research in Support of the Airborne Laser* [4] the Global Aerosol Data Set (GADS) [5], and Air Force Weather Agency numerical weather forecasting data. GADS provides aerosol constituent number densities on a $5° \times 5°$ grid worldwide. ExPERT mapping software allows the HELEEOS operator to choose from specific site or regional surface and upper air data to characterize correlated molecular absorption, aerosol absorption and scattering by percentile. The PDF nature

of the HELEEOS atmospheric effects package enables realistic probabilistic outcome analyses which permit an estimation of the level of uncertainty in the calculated probability of effect (P_e). HELEEOS users can additionally access, display and export the atmospheric data independent of a HEL engagement simulation [6]. Integration of the Surface Marine Gridded Climatology (SMGC) v2.0 database, the Advanced Navy Aerosol Model (ANAM) [7], and the Navy Surface Layer Optical Turbulence (NSLOT) model [8] provides worldwide coverage over all ocean regions on a $1° \times 1°$ grid. Molecular scattering is computed based on Rayleigh theory. Molecular absorption effects are computed for the top 13 absorbing species using line strength information from the HITRAN 2004 database [9] in conjunction with a community standard molecular absorption continuum code. Aerosol scattering and absorption are computed with the Wiscombe Mie model [10].

Vertical profiles of molecular absorption and molecular scattering can be defined in a number of ways in HELEEOS. Thirteen standard atmospheres representing summer and winter conditions for the major climate regions are available. In addition, a large number of specific worldwide surface locations defined in ExPERT, as well as any ocean location on the $1° \times 1°$ latitude/longitude grid, can be selected.

The red circles in Fig. 1 indicate the 408 ground sites available from ExPERT in HELEEOS. The user can also select from one of nine relative humidity percentile conditions (ranging from 1st to 99th percentiles) to model, with the default being 50th percentile conditions, as well as time of day in 3 h local time blocks for any of these sites.

A diverse array of aerosol vertical profiles is also available. There are 10 profiles defined using the Optical Properties of Aerosols and Clouds (OPAC) [11] code, three MODTRAN aerosol profiles [12], and the windspeed-driven aerosol mixtures from ANAM. The aerosol profile for each ExPERT site is defined using the constituent data from GADS.

HELEEOS allows the definition of five liquid water cloud types, three cirrus (ice) cloud types, five rain rates, fog, ice fog, and drizzle. The clouds and fog are microphysically characterized using OPAC, while the rain cases (with the exception of drizzle) are defined using a Marshall–Palmer distribution [13].

Several optical turbulence profiles are available in the model, for example, Hufnagel–Valley 5/7 [14] and Clear 1 [15]. The climatological C_n^2 profile is a unique feature of HELEEOS. It combines the extensive climatological record of the ExPERT database with the optical turbulence data of the *Master Database for Optical Turbulence Research in Support of the Airborne Laser*. The optical turbulence database is a direct compilation of many worldwide night-time thermosonde campaigns. Each climatological C_n^2 profile is tailored to individual sites by distinctly referencing the optical turbulence database based on user-selected surface relative humidities. HELEEOS physically correlates
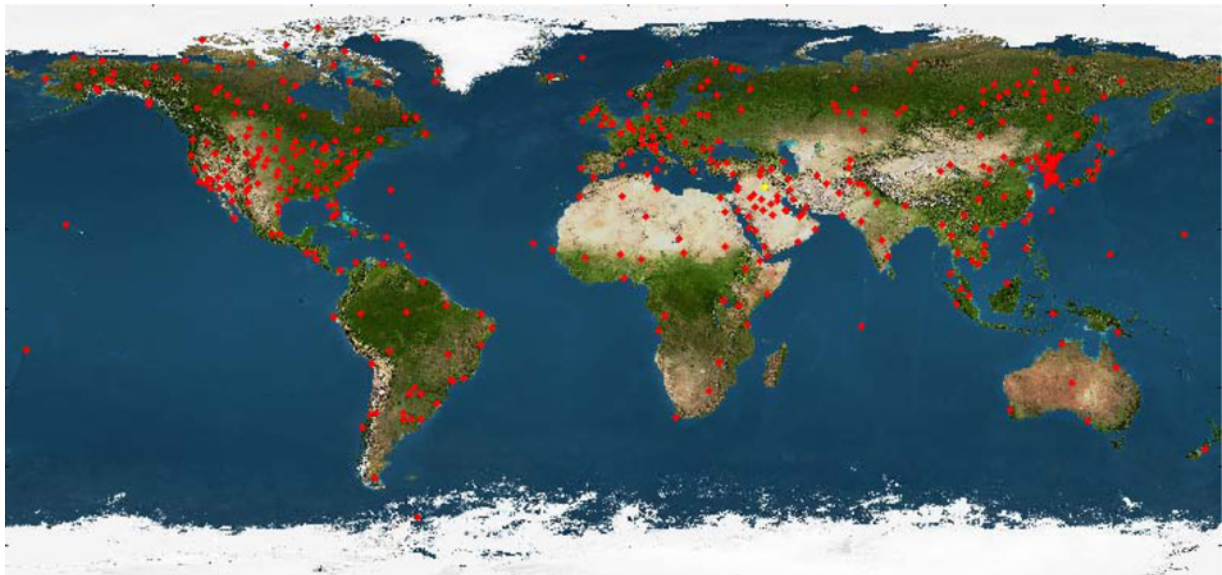
Fig. 1 Four hundred and eight worldwide land locations available in HELEEOS.

temperature and relative humidity percentiles to corresponding percentage values in the optical turbulence database. Within the boundary layer, HELEEOS correlates the optical turbulence profiles to percentiles of relative humidity, and in the free atmosphere to standard atmosphere temperatures percentiles. These physical correlations to probabilistic climatology form the basis of the climatological C_n^2 profiles, a feature unique to the HELEEOS engagement package [16]. Over the first 50 m of the ocean surface, HELEEOS employs the NSLOT model. Above the lowest 50 m, the Hufnagel–Valley 5/7 model is used to define over-ocean C_n^2 values.

Probability of cloud free line of sight (CFLOS) is incorporated into HELEEOS for air-to-air, air-to-ground, and ground-to-air (or space) look angles at most of the 400+ ExPERT land sites. The air-to-air and air-to-ground CFLOS probabilities are obtained via an integration of Air Force Combat Climatology Center (AFCCC) ground-to-space CFLOS tables with AFCCC ceiling height data [17].

HELEEOS supports any user-defined wavelength from 0.40 μm to 8.6 m, with 24 specific wavelengths typically associated with laser operation available via lookup table for minimum run-time.

II.   Methodology

In the current study the capabilities of the HELEEOS model are exploited to study the worldwide variance in low altitude laser system performance across a broad range of atmospheric conditions, based on both statistical historical data and weather reanalysis data, under the assumption of clear air aerosols for two wavelengths often considered for high energy applications. Both 0300–0600 and 1500–1800 local time blocks are analyzed for summer and winter conditions for the probabilistic climatology (historical statistical) data, and 0600 and 1800 Universal Coordinated Time (UTC) for 15 January 2007 and 15 July 2007 for the NCEP/NCAR weather reanalysis data. Overall Strehl Ratio, the ratio of atmospherically attenuated propagation to that of diffraction limited propagation, is the primary performance metric used in the study. Diffraction limited propagation is laser energy that is only affected by the unavoidable effects of diffraction caused by the optical system; it is the absolute best case scenario. Atmospherically attenuated propagation includes the deleterious effects of the real atmosphere. Thus an atmosphere that affects the laser propagation minimally will produce a Strehl Ratio near 1. In general, higher Strehl Ratios—values closer to 1—mean shorter required dwell times and longer effective ranges. Results are presented as color-coded maps, based on wavelength.

Parameters used throughout the study include:
- Aperture: 0.5 m diameter, circular, uniform beam with 0.1 relative central obscuration
- Turbulence conditions: Correlated climatological C_n^2, mode value, for land sites, and NSLOT model for the ocean sites
- Tilt-only correction; no adaptive optics
- No jitter

Parameters varied as part of the study are as follows:
- Two wavelengths: 1.0642 μm and 1.31525 μm
- Two hundred and thirty three ExPERT surface locations worldwide, located north of 12°N latitude and between 130°W longitude and 70°E longitude; shown in Fig. 2
- Oceanic locations on a 1° × 1° latitude/longitude grid within the same latitude and longitude limits, approximately 6000 sites
- Atmospheric conditions:
  - 50th percentile relative humidity conditions for climatological data
  - 0300–0600, 1500–1800 local time blocks for all land sites for climatological data
  - Boundary layer height varying from 500 m to 1524 m, dependent upon season and time of day
  - Summer and winter
  - Clear sky aerosols
- Geometry, illustrated in Fig. 3:
  - Air-to-Surface, 2000 m slant range:
    - Platform (laser) altitude 500 m
    - Target altitude 0 m
   - Platform velocity 100 m s^{-1} toward stationary target
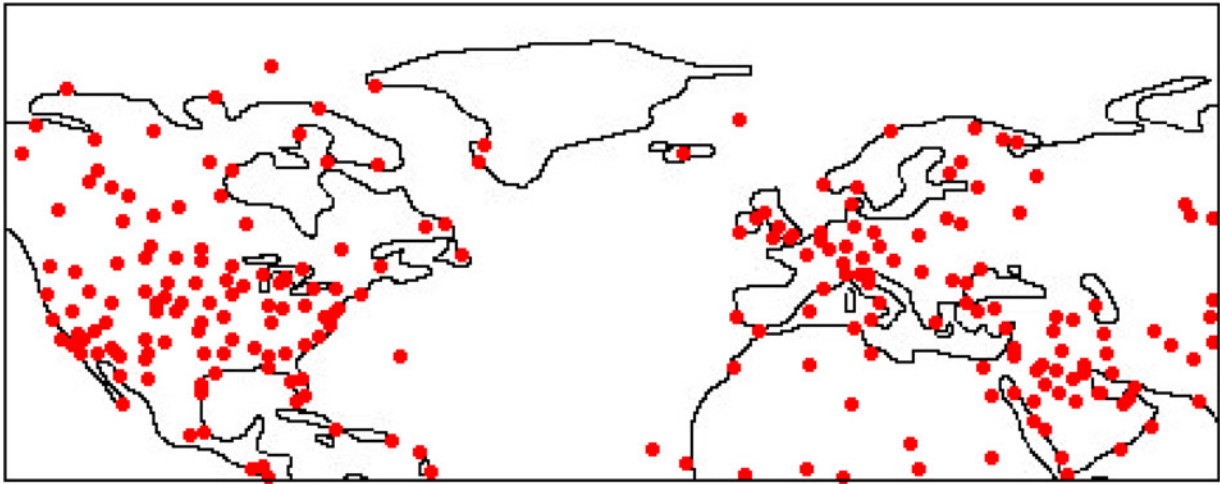
Fig. 2 Geographic area evaluated in the current study, includes 233 ExPERT land sites and approximately 6000 ocean locations.

In previous analyses, HELEEOS has been used to analyze various aspects of worldwide performance based on the climatological model [18,19]. In this study, climatological results are compared with weather reanalysis data results, available from NCEP, for specific dates and times, for the first time.

The current study concentrates on a large portion of the northern hemisphere, north of 12°N latitude and between 130°W longitude and 70°E longitude. This region contains 233 largely midlatitude and desert ExPERT locations and approximately 6000 ocean locations under summer conditions. The number of ocean locations is somewhat lower in winter due to lack of reported data from icebound areas. The 233 ExPERT sites are illustrated in Fig. 2.

A very low altitude oblique engagement geometry is the focus of the current study. A platform altitude of 500 m and a platform velocity of $100 \, \text{m s}^{-1}$ to the north are used throughout, with a stationary target located to the north of the platform (relative azimuth of 0°) at a slant range of 2000 m. The wind is allowed to vary in direction and speed according to climatology or specific NCEP data. This engagement geometry is depicted in Fig. 3. The HELEEOS performance model has been shown to be comparable to wave-optics within approximately ±10% for these types of geometries and output powers [20]. The relatively slow platform velocity of $100 \, \text{m s}^{-1}$ is assumed due to the low altitude of the engagement. If the platform velocity is increased, there would be only a small mitigating effect on beam spread due to thermal blooming as the highly oblique geometry would cause most of the increased effective air
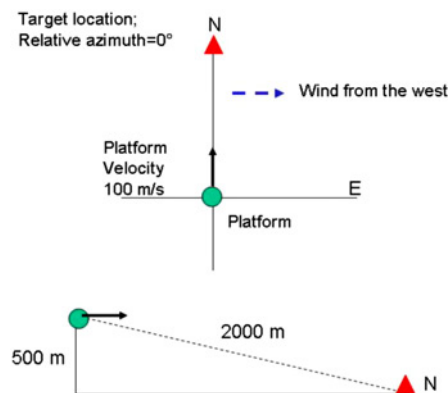
Fig. 3 Engagement geometry evaluated in the current study with top view (top) and side view (bottom); wind is shown from the west in this schematic.

flow to blow along the beam rather than across it. The 500 m platform height is used because this height is generally well within the atmospheric boundary layer, which is the lowest well-mixed 500–2000 m of the atmosphere and is strongly characterized by air interaction with the ground or ocean surface.

Figures 4 and 5 summarize, respectively, climatological and NCEP values for the geographic region of interest of surface air temperature (C), air-sea temperature difference (C), wind speed (m s^{-1}), and relative humidity (%), for January, 1500–1800 local time. In the case of the NCEP values, the data are specifically for 15 January 2007, 1800 UTC. This particular season/local time combination is presented as illustrative of climatological and NCEP value comparisons. While the climatological data are always 1500–1800 local time, the NCEP data vary approximately ±6 h from 1800 local time based on longitude within the region of interest. The climatological data are 50th percentile relative humidity conditions for the ExPERT sites for January for the 1500–1800 local time block and mean values for all parameters for January for the ocean locations. In both cases sea temperature data from the SMGC database are used in computing air-sea temperature difference. In addition, in both cases the definition of aerosol constituents and corresponding number densities for the ExPERT land sites is provided by GADS, and aerosols for ocean locations are defined using ANAM.

The NCEP values, being single realizations in time, exhibit considerably more spatial (geographic) complexity, featuring changes in values over relatively small distances, than the highly averaged climatological values. This greater degree of complexity is manifest in the Strehl Ratio results of the current study. The lack of ship-based reporting from ice-bound areas is evident in the climatological values by missing data from the Arctic Ocean and Hudson Bay. This lack of data at extreme northern over water latitudes is also evident in the NCEP air-sea temperature difference plot. Also, the NCEP relative humidity values for many ExPERT locations for this time block, particularly in North America, are greater than the 50th percentile climatological relative humidity values, indicating the actual conditions of 15 January 2007/1800 UTC are more stressing, particularly for aerosol effects at many locations, than average.

For the climatological cases, surface wind vectors are derived from a 60-year weather reanalysis climatology. These wind data are available every 2.5° by 2.5° latitude/longitude over the globe. Areas of light surface winds, over land or water, strongly impact the effect of thermal blooming in the stressing engagement geometry used for this study.

III.   Results

A large number of comparisons can be made from the available data. Figure 6 compares total Strehl Ratio results for 1.0642 μm and 1.31525 μm for the climatological case, for January, 1500–1800 local time. This low altitude oblique engagement geometry featuring relatively low effective wind is stressing for both wavelengths, with Strehl Ratios no higher than approximately 0.4 for either wavelength for these engagement decisions. In general Strehl Ratios are higher for 1.0642 μm, due to the much greater impact of thermal blooming due to water vapor absorption in the lower atmosphere at 1.31525 μm. Comparing Fig. 6 with Fig. 4, general trends of how climatic conditions impact estimates of HEL system performance may be discerned. The broad areas in the central Atlantic featuring relatively high Strehl Ratio at 1.0642 μm correspond to areas of near zero air-sea temperature difference which results in very benign (weak) turbulence conditions predicted by NSLOT. The area of lower Strehl Ratio at 1.0642 μm off the northeast coast of the United States corresponds to an area of both more negative air-sea temperature difference and higher relative humidity, both of which decrease performance. The more negative air-sea temperature difference results in significantly higher optical turbulence estimates from NSLOT and the higher relative humidity leads to greater aerosol size distributions and aerosol extinction. The band of slightly improved Strehl Ratio for 1.31525 μm off the east central coast of the United States is an area of greater turbulence strength caused by the air-sea temperature differences associated with the Gulf Stream. This area of somewhat increased optical turbulence actually mitigates some of the effects of thermal blooming.

Another interesting aspect of the plots in Fig. 6 is the east–west line of lower Strehl Ratios off the east coast of Florida into the central Atlantic. This line of lower Strehl Ratios is due to enhanced thermal blooming caused by light climatological winds out of the south (see Fig. 4). Light southerly winds run along the engagement geometry for this study (see Fig. 3). This limits the amount of aspiration (cooling) that crosses the laser beam and enhances thermal blooming.
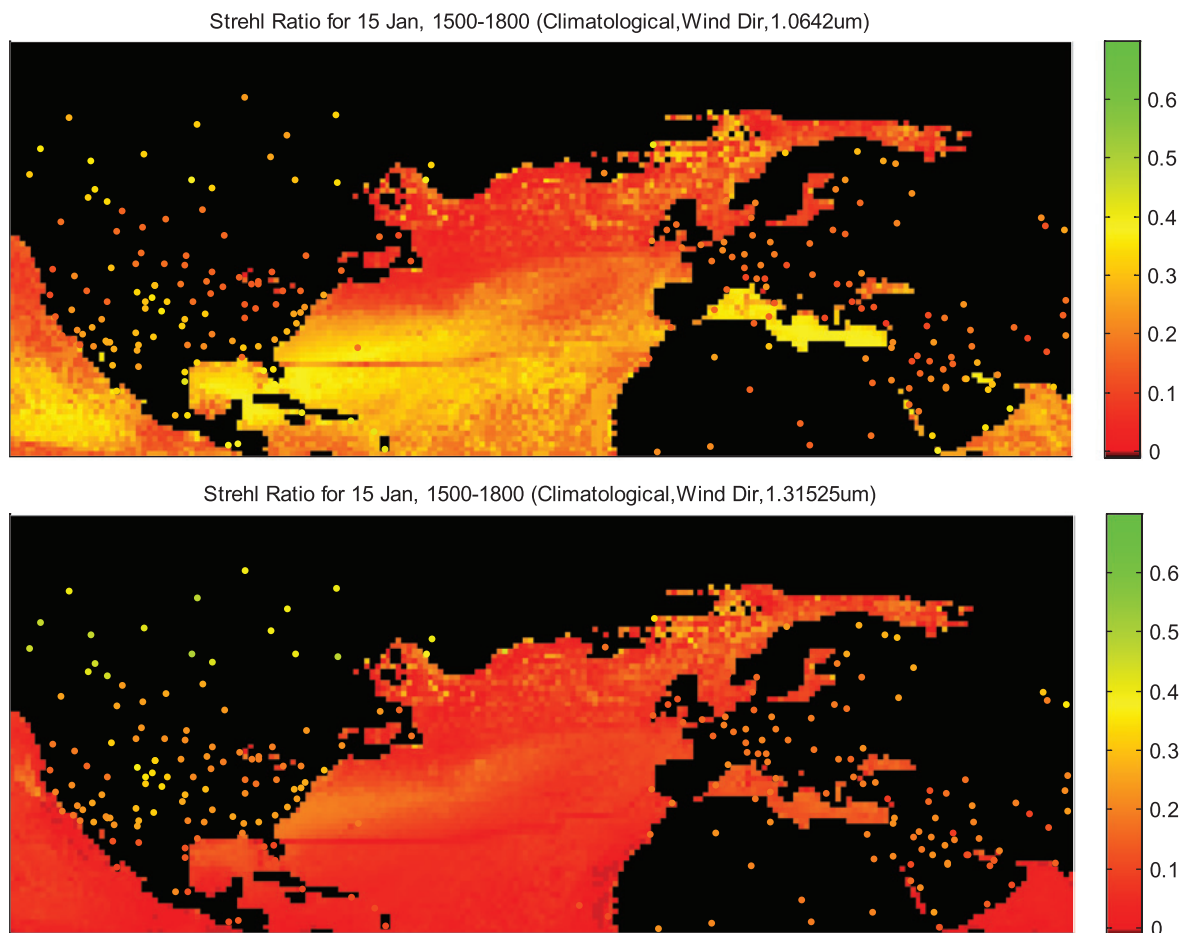
496
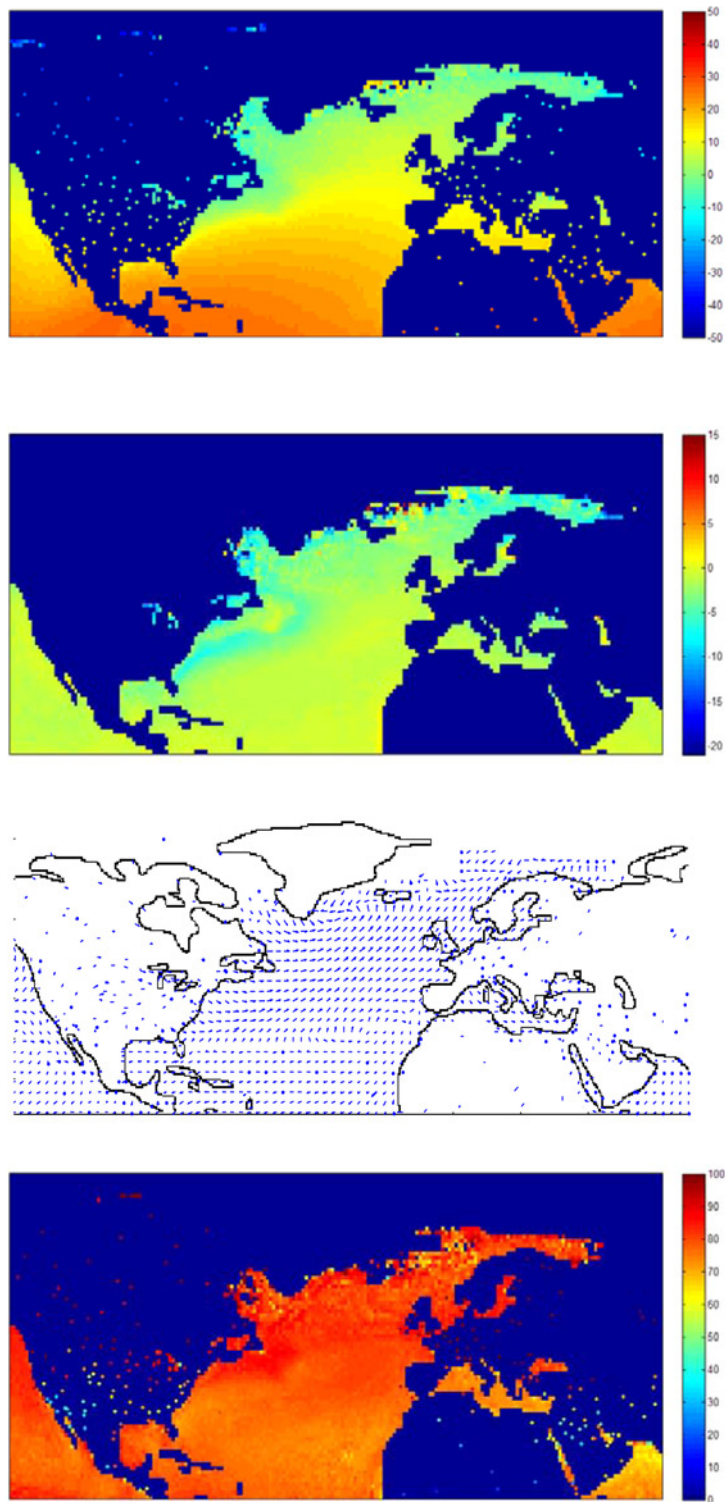
Fig. 4 Climatological values for (top to bottom) air temperature, air-sea temperature difference, wind speed and direction, and relative humidity, January, 1500–1800 local time.
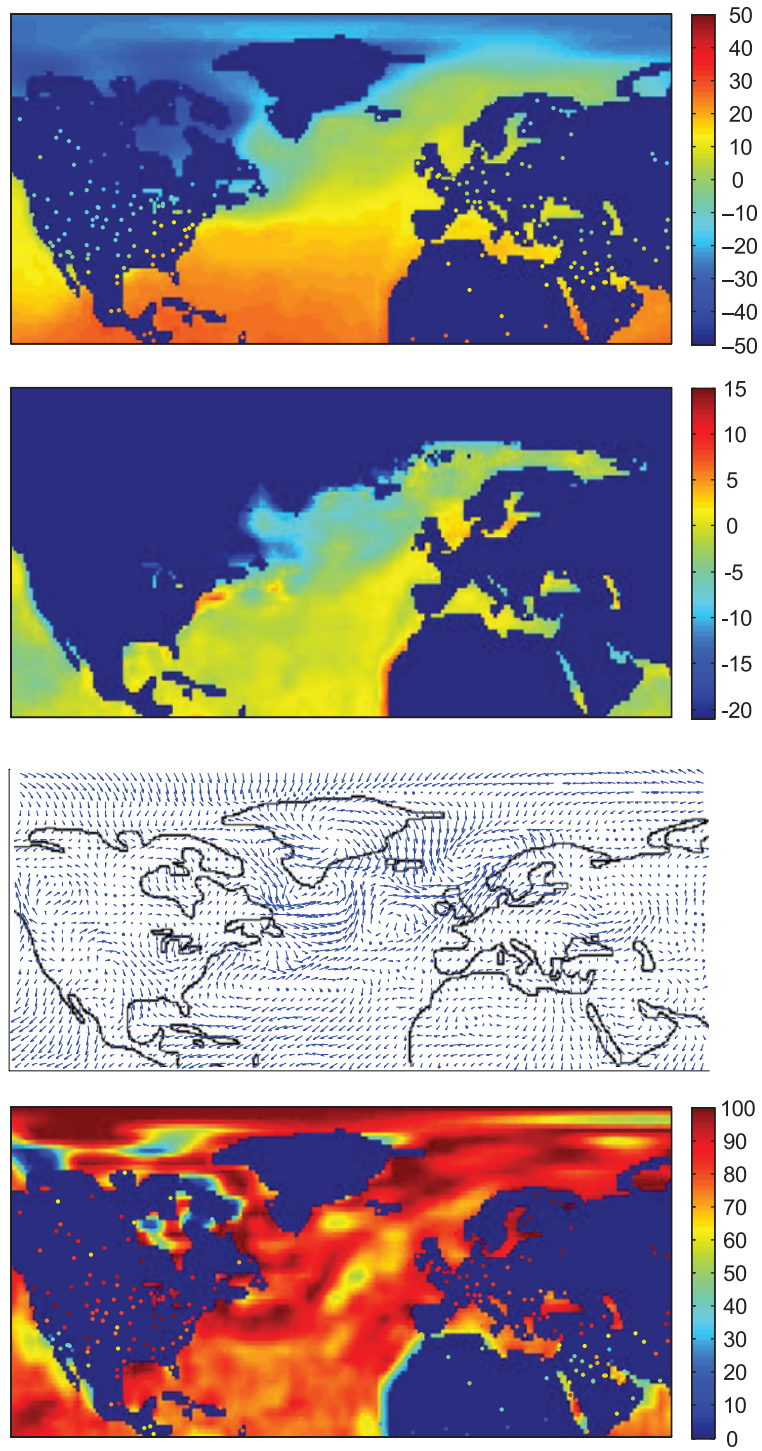
Fig. 5 NCEP values for (top to bottom) air temperature, air-sea temperature difference, wind speed and direction, and relative humidity, 15 January 2007, 1800 UTC.

Strehl Ratio for 15 Jan, 1500-1800 (Climatological,Wind Dir,1.0642um)

Strehl Ratio for 15 Jan, 1500-1800 (Climatological,Wind Dir,1.31525um)
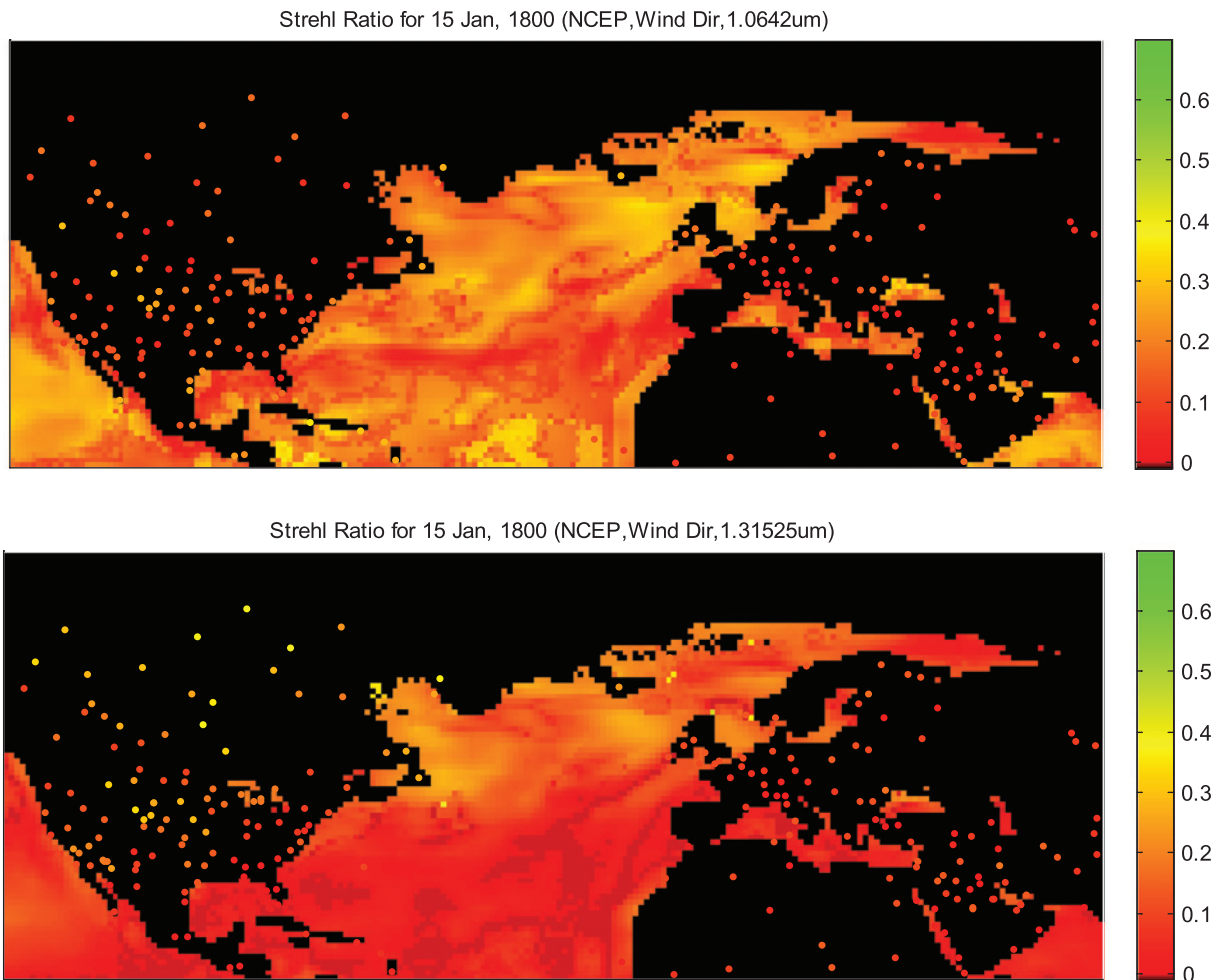

Fig. 6 Total Strehl Ratio at 1.0642 μm (top) and 1.31525 μm (bottom), based on climatological data, January, 1500–1800 local time.

Figure 7 compares total Strehl Ratio results for 1.0642 μm and 1.31525 μm for the NCEP case, for 15 January 2007, 1800 UTC. Comparing with Fig. 6, particularly for 1.0642 μm (top plot in each figure) considerably more complex structure in the results over the oceans is evident, though the range of Strehl Ratio values is approximately the same.

The lower Strehl Ratio results for the NCEP data for the majority of ExPERT locations as compared with the climatological case of Fig. 6 are directly attributable to generally higher relative humidity (RH) values over the land sites in the NCEP data. Higher relative humidity causes water soluble aerosols to increase in size and create more aerosol extinction.

Several specific observations can be made. The band of sharply lower Strehl Ratio for both wavelengths stretching southwestward from Ireland is due to particularly low surface winds, exacerbating thermal blooming. Referring to Fig. 5, the improved Strehl Ratio in the north Atlantic at 1.31525 μm is due to a combination of sharply reduced temperatures, which lowers the absolute humidity, and generally higher wind speeds. While higher wind speeds result in greater aerosol extinction using ANAM, this greater loss mostly due to scattering has a somewhat mitigating effect on thermal blooming. Overall performance can improve if the wind speed is not too great, an example of degrading atmospheric effects which, when they coexist, might be exploited if properly forecast.

Figure 8 compares total Strehl Ratio results for 1.0642 μm for the NCEP case, for 15 January 2007, 1800 UTC and 15 July 2007, 1800 UTC, providing a winter–summer comparison. Winter conditions are generally somewhat more favorable. This difference is attributable to a large extent to lower surface wind speeds in the summer, resulting in a general increase in thermal blooming; and to higher summer absolute humidity causing greater continuum

Strehl Ratio for 15 Jan, 1800 (NCEP,Wind Dir,1.0642um)

Strehl Ratio for 15 Jan, 1800 (NCEP,Wind Dir,1.31525um)

Fig. 7 Total Strehl Ratio at 1.0642 μm (top) and 1.31525 μm (bottom), based on NCEP data, 15 January 2007, 1800 UTC.

absorption and thermal blooming. Overall turbulence effects are actually more benign on 15 July 2007 for both land and ocean locations, however this also in turn produces somewhat greater thermal blooming effects for this engagement geometry.

The V-shaped region of lower Strehl Ratio on 15 July 0600 UTC in the central Atlantic is due once again to particularly low surface winds.

The top panels of Figs. 7 and 8 allow a time of day comparison for the NCEP case, 1800 UTC vs 0600 UTC, respectively. While global performance remains approximately the same, there are operationally pertinent changes in localized areas across these 12 h. For example, conditions southeast of Newfoundland noticeably improve at 1800 UTC, likely due to changes in wind speed and direction. This is another example of meteorological effects which might be exploited for operational advantage if correctly forecast.

Figure 9 compares total Strehl Ratio results for 1.0642 μm for the NCEP case, for 15 January 2007, 0600 UTC and Strehl Ratio for all effects except thermal blooming, for the same date and time. The top panel here is the same as that in Fig. 8. Figure 9 clearly illustrates the dominate effect of thermal blooming on overall system performance. The regions of particularly low total Strehl Ratio (top panel) in the central Atlantic correspond to areas of very low surface winds.
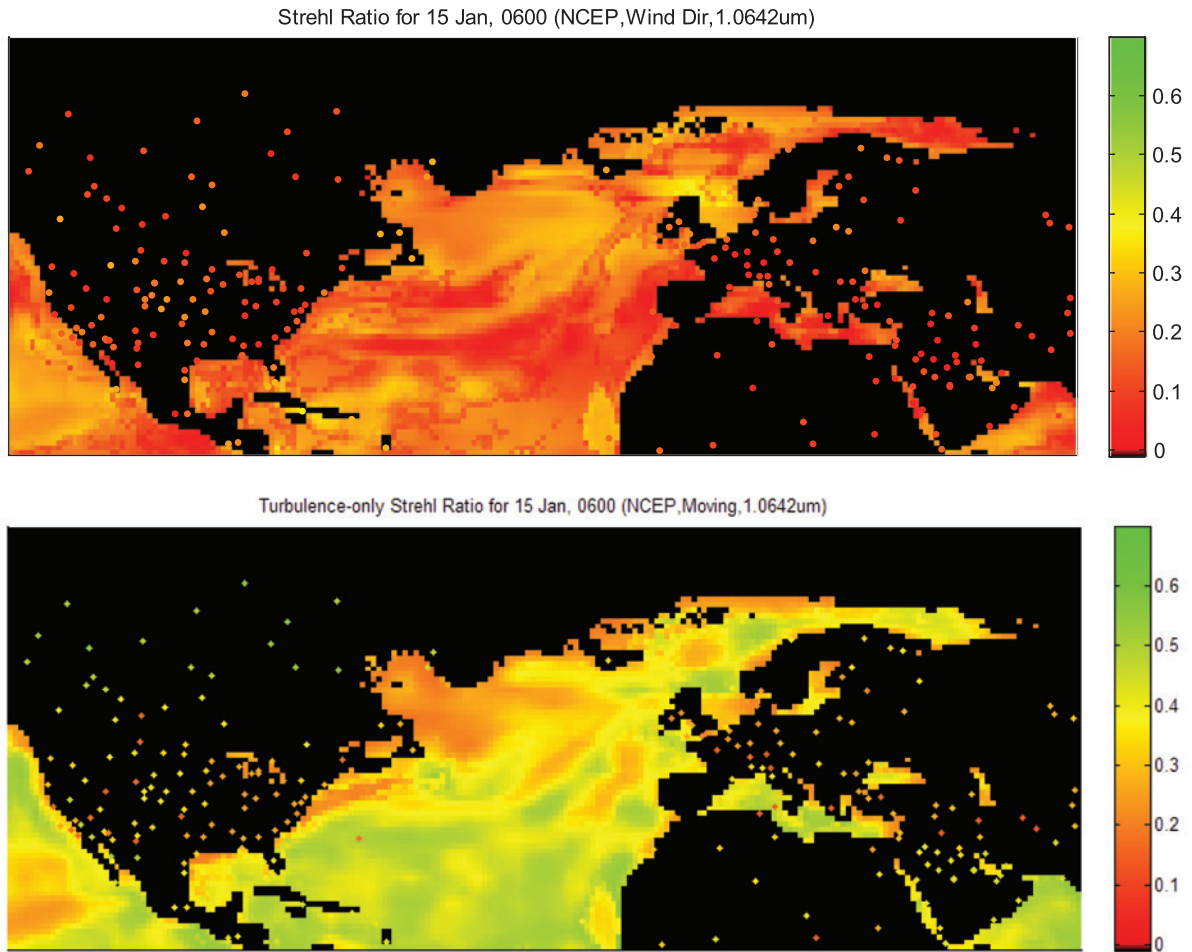
Strehl Ratio for 15 Jan, 0600 (NCEP,Wind Dir,1.0642um)

Strehl Ratio for 15 July, 0600 (NCEP,Wind Dir,1.0642um)
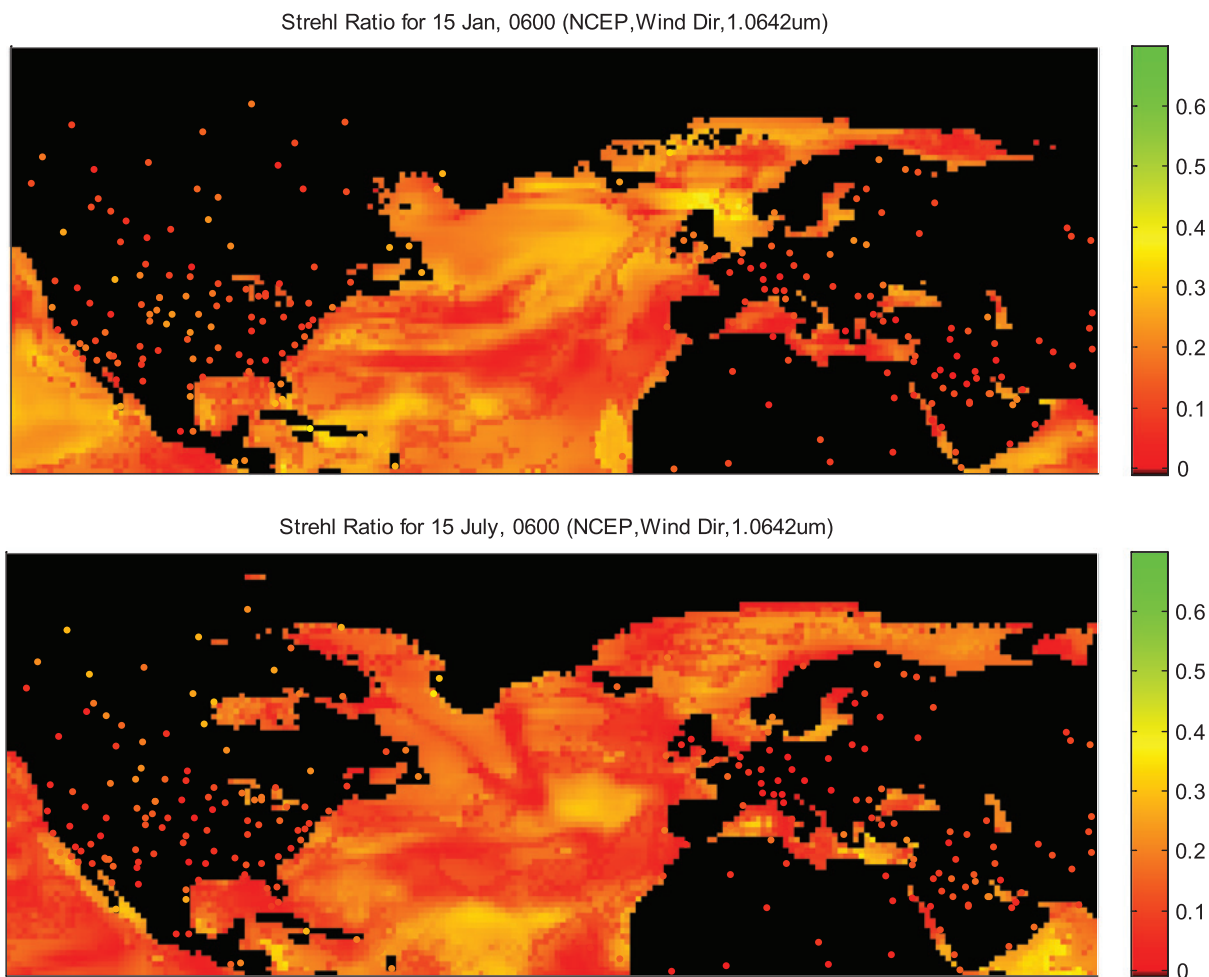
Fig. 8 Total Strehl Ratio at 1.0642 μm winter, 15 January 2007 (top) and summer, 15 July 2007 (bottom), based on NCEP data, 0600 local time.

In the bottom panel where thermal blooming effects are removed, the reduced performance over the ocean northeast of Newfoundland and northwest of Iceland is due to high surface winds which produce more sea-salt aerosols and more aerosol extinction. The region of low performance in the lower panel southwest of Baja California is due to distinctly negative air-sea temperature differences, which result in stronger turbulence. However, this same region exhibits relatively good performance if thermal blooming is considered, due to the somewhat mitigating effect of the beam spread due to turbulence on blooming. The same thing is true off the west coast of Africa.

There are, without doubt, distinct tradeoffs in system performance between thermal blooming and other effects generally considered as losses, for example aerosol extinction and beam spread due to turbulence, which vary as a function of engagement parameters which must be fully understood in order to maximize operational performance.

Figure 10 compares total Strehl Ratio results for 1.0642 μm and 1.31525 μm for the climatological case, for January, 0300–0600 local time. Of interest in this comparison is the similar performance predicted for the two wavelengths for many of the land sites, for example Wright-Patterson AFB, Ohio. For the climatological case, surface winds are in general very light at 0300–0600 local time for all locations and therefore do not contribute significantly to variations in predicted performance. Figure 11 plots atmospheric extinction effects, both absorption and scattering, as a function of altitude for 1.0642 μm and 1.31525 μm for Wright-Patterson AFB, Ohio, based on climatological data for January, 0300–0600 local time. Figure 11 illustrates that while absorption is greater

Strehl Ratio for 15 Jan, 0600 (NCEP,Wind Dir,1.0642um)

Turbulence-only Strehl Ratio for 15 Jan, 0600 (NCEP,Moving,1.0642um)

Fig. 9 Total Strehl Ratio at 1.0642 μm winter, 15 January 2007 (top) and Strehl Ratio without thermal blooming at 1.0642 μm winter, 15 January 2007 (bottom), based on NCEP data, 0600 UTC.

at 1.31525 μm, aerosol scattering and total extinction is distinctly greater at 1.0642 μm because is it a shorter wavelength. This larger extinction at 1.0642 μm leads, for this low altitude oblique geometry, to approximately the same overall Strehl Ratio, even though thermal blooming beam spread is greater at 1.31525 μm. While 1.0642 μm is relatively clean in terms of molecular absorption lines, there remains primarily continuum absorption, and an aerosol absorption component. The resulting total absorption is sufficient to result in blooming for this engagement. Figure 11 also illustrates the increased aerosol scattering with height within the atmospheric boundary captured by HELEEOS, the correct representation of which is important in evaluation of the expected outcome of low altitude engagements [18].

IV. Conclusions

Government-developed tools exist for analysis of laser weapon system performance on a worldwide basis. For the first time the use of gridded weather reanalysis data with a directed energy performance model has been demonstrated, constituting a first step toward development of a low altitude, tactical directed energy mission planning capability. This effort essentially begins the process of validating HELEEOS as a tactical decision aid for the operational employment of high energy laser systems. The Air Force weather community has in the past operationally employed such tactical decision aids for the support of precision-guided munitions and other electro-optical systems [21]. A
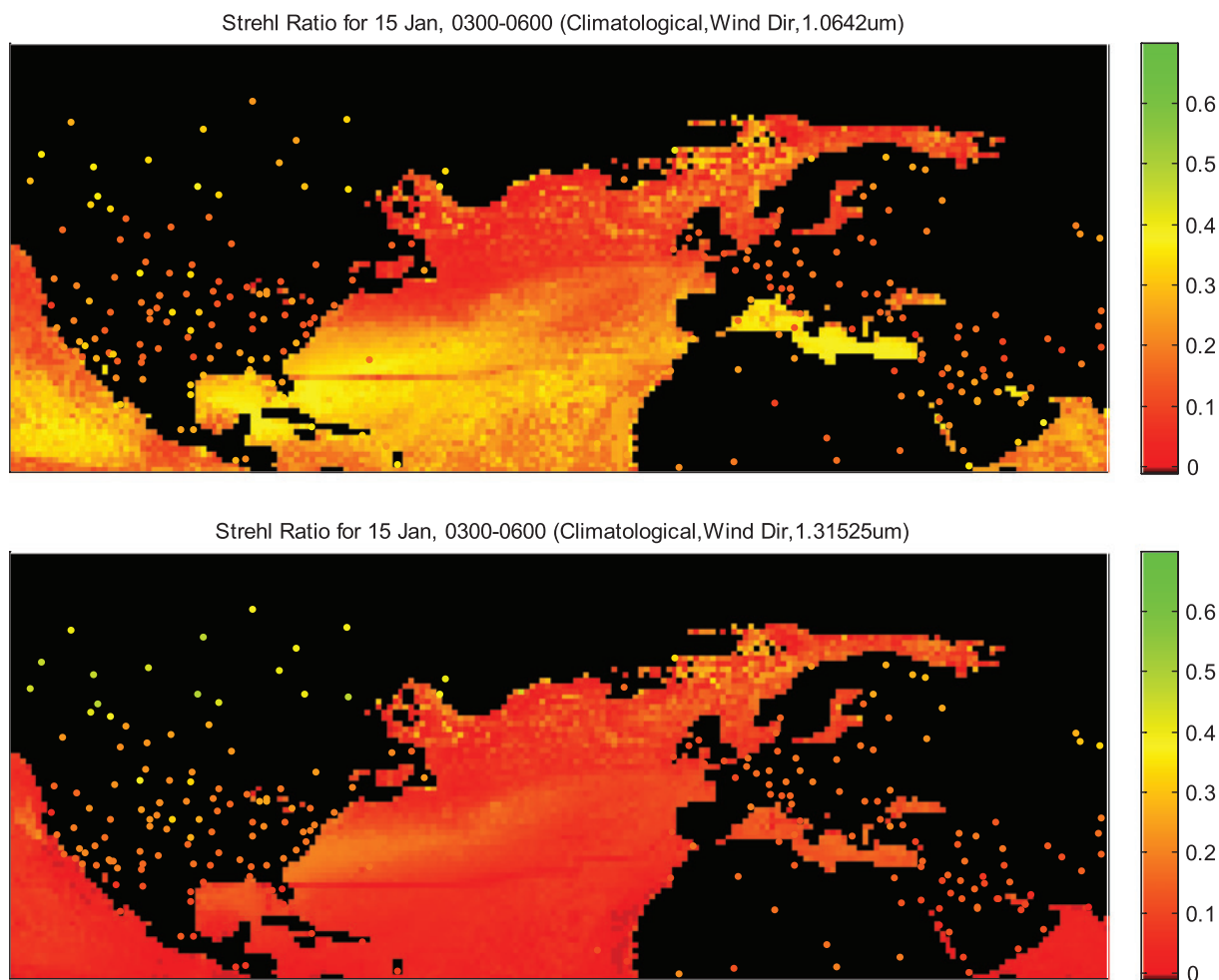
Fig. 10 Total Strehl Ratio at 1.0642 μm (top) and 1.31525 μm (bottom) based on climatological data, January, 0300–0600 local time block.
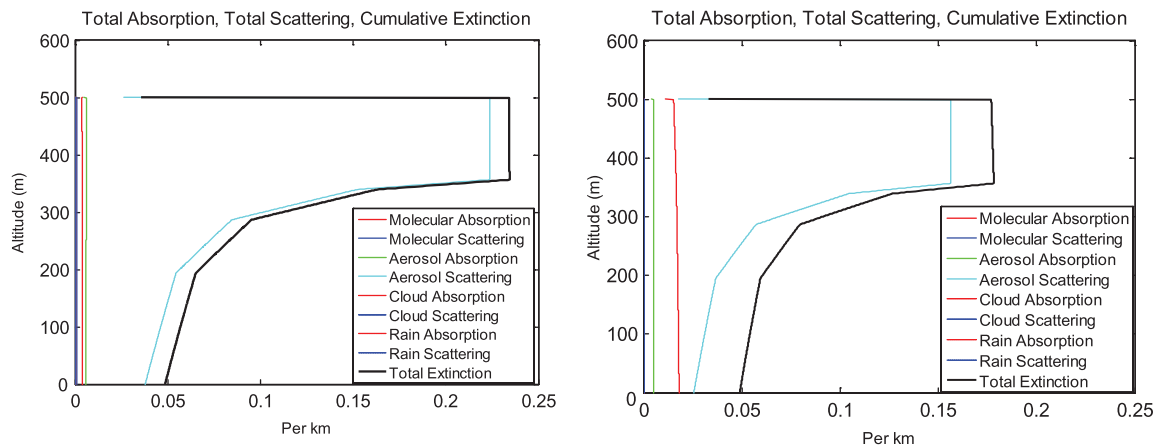
Fig. 11 Wright-Patterson AFB, Ohio, winter (January), 0600–0900 local time, 50th percentile RH, (1.0642 μm) on the left, (1.31525 μm) on the right.

HELEEOS tactical decision aid would be useful for Air Force weather community and support of DoD directed energy weapons systems.

Complex interactions between the effects of meteorological parameters as a function of location, specific time of day, and season on predicted laser system performance have been demonstrated. There are distinct tradeoffs in system performance between thermal blooming and other effects generally considered as losses, for example beam spread due to turbulence and aerosol extinction, which vary as a function of engagement parameters which must be fully understood in order to maximize operational performance. Use of numerical reanalysis data reveals operationally relevant changes in predicted system performance over fairly localized areas, indicating that in many cases conditions exist that might be exploited for operational advantage in employment of directed energy weapons if correctly forecast and analyzed.

Acknowledgments

References

[1] Kalnay, E., Kanamitsu, M., Kistler, R., Collins, W., Deaven, D., Gandin, L., Iredell, M., Saha, S., White, G., Woollen, J., Zhu, Y., Leetmaa, A., Reynolds, B., Chelliah, M., Ebisuzaki, W., Higgins, W., Janowiak, J., Mo, K., Ropelewski, C., Wang, J., Jenne, R., and Joseph, D., "The NCEP/NCAR 40-Year Reanalysis Project," *Bulletin of the American Meteorological Society*, Vol. 77, 1996, pp. 437–471.
doi: 10.1175/1520-0477(1996)077<0437:TNYRP>2.0.CO;2

[2] Bartell, R. J., Perram, G. P., Fiorino, S. T., Long, S. N., Houle, M. J., Rice, C. A., Manning, Z. P., Krizo, M. J., Bunch, D. W., and Gravley, L. E., "Methodology for Comparing Worldwide Performance of Diverse Weight-Constrained High Energy Laser Systems," *Proceeding of the SPIE*, Vol. 5792, Orlando, FL, March 2005, p. 76.

[3] Squires, M. F., Bietler, B. A., Fiorino, S. T., Parks, D. L., Youkhana, F. W., and Smith, H. D., "A Method for Creating Regional and Worldwide Datasets of Extreme and Average Values," *Institute of Environmental Sciences 1995 Proceedings, 41st Annual Meeting*, Mount Prospect, IL, 1995.

[4] Bussey, A. J., Roadcap, J. R., Beland, R. R., and Jumper, G. Y., "Master Database for Optical Turbulence Research in Support of Airborne Laser," Air Force Research Lab. TR, AFRL-VS-TR-2000-1545, 2000.

[5] Koepke, P., Hess, Schult, M. I., and Shettle, E. P., "Global Aerosol Data Set," MPI Meteorologie Hamburg, Rept. No. 243, 1997, 44 pp.

[6] Fiorino, S. T., Bartell, R. J., Perram, G. P., Bunch, D. W., Gravley, L. E., Rice, C. A., Manning, Z. P., and Krizo, M. J., "The HELEEOS Atmospheric Effects Package: A Probabilistic Method for Evaluating Uncertainty in Low-Altitude High Energy Laser Effectiveness," *Journal of Directed Energy*, Vol. 1, No. 4, 2006, pp. 347–360.

[7] Gathman, S. G., van Eijk, A. M. J., Cohen, L. H., "Characterizing Large Aerosols in the Lowest Levels of the Marine Atmosphere," *Proceedings of the SPIE*, Vol. 3433, 1998, pp. 41–52.

[8] Frederickson, P. A., Davidson, K. L., Zeisse, C. R., and Bendall, C. S., "Estimates of the Refractive Index Structure Parameter (C_n^2) over the Ocean Using Bulk Methods," *Journal of Applied Meteorology*, Vol. 39, 2000, p. 1770.

[9] Rothmanan, L. S., Jacquemart, D., Barbe, A., Chris Benner, D., Birk, M., Browne, L. R., Carleer, M. R., Chackerian Jr., C., Chance, K., Coudert, L. H., Dana, V., Devi, V. M., Flaud, J. -M., Gamache, R. R., Goldman, A., Hartmann, J. -M., Jucks, K. W., Maki, A. G., Mandin, J. -Y., Massie, S. T., Orphal, J., Perrin, A., Rinsland, C. P., Smith, M. A. H., Tennyson, J., Tolchenov, R. N., Toth, R. A., Vander Auwera, J., Varanasi, P., and Wagner, G., "The HITRAN 2004 Molecular Spectroscopic Database," *Journal of Quantitative Spectroscopy and Radiative Transfer*, Vol. 96, 2005, pp. 139–204.

[10] Wiscombe, W. J., "Improved Mie Scattering Algorithms," *Applied Optics*, Vol. 19, No. 9, 1980, pp. 1505–1510.
doi: 10.1364/AO.19.001505

[11] Hess, M., Koepke, P., and Schult, I., "Optical Properties of Aerosols and Clouds: the Software Package OPAC," *Bulletin of the American Meteorological Society*, Vol. 79, 1998, pp. 831–844.
doi: 10.1175/1520-0477(1998)079<0831:OPOAAC>2.0.CO;2

[12] Shettle, E. P., and Fenn, R. W., "Models for the Aerosols of the Lower Atmosphere and the Effects of Humidity Variations on their Optical Properties," Air Force Geophysics Lab. TR, AFGL-TR-79-0214, 1979.

[13] Marshall, J. S., and Palmer, W. McK., "The Distribution of Raindrops with Size," *Journal of the Atmospheric Sciences*, Vol. 5, 1948, pp. 165–166.
doi: 10.1175/1520-0469(1948)005<0165:TDORWS>2.0.CO;2

[14] Hufnagel, R. E., "Propagation Through Atmospheric Turbulence," *The Infrared Handbook*, edited by W. L. Wolfe, and G. J. Zissis, Infrared Information Analysis Center, Ann Arbor, MI, 1985.

[15] Beland, R. R., "Propagation Through Atmospheric Optical Turbulence," *Atmospheric Propagation of Radiation*, edited by F. G. Smith, SPIE, Bellingham, WA, 1993, pp. 157–232.

[16] Gravley, L. E., Fiorino, S. T., Bartell, R. J., Perram, G. P., Krizo, M. J., and Le, K. B., "Comparison of Climatological Optical Turbulence Profiles to Standard, Statistical and Numerical Models using HELEEOS," *Journal of Directed Energy*, Vol. 2, No. 4, pp. 347–362.

[17] Fiorino, S. T., Bartell, R. J., Eckel, J. D., Krizo, M. J., and Cusumano, S. J., "Application and Impacts of Ground-to-Space Cloud Free Line of Sight Probabilities to Air-to-Ground High Energy Laser Engagement Scenarios," *Directed Energy Professional Society 9th Annual DE Symposium*, Albuquerque, NM, 30 Oct.–2 Nov. 2006.

[18] Fiorino, S.T., Bartell, R. J., Krizo, M. J., and Cusumano, S. J., "Expected Worldwide, Low-Altitude Laser Performance in the Presence of Common Atmospheric Obscurants," *Journal of Directed Energy*, Vol. 2, No. 4, 2007, pp. 363–375.

[19] Fiorino, S. T., Bartell, R. J., Perram, G. P., Krizo, M. J., Fedyk, D. J., Wisdom, B. W., and Cusumano, S. J., "Worldwide Estimates and Uncertainty Assessments of Laser Propagation for Diverse Geometries for Paths in the Altitude Regime of 3 km and Below at Wavelengths of 0.355 μm to 10.6 μm," *Proceedings of the SPIE*, Vol. 6551-03, Orlando, FL, April 2007.

[20] Bartell, R. J., Fiorino, S. T., Krizo, M. J., Perram, G. P., Huster, T., Cheney, J., Magee, E., Whiteley, M., and Ngwele, A., "Comparison of Peak Irradiance and Power-in-the-Bucket Predictions Among Several Scaling Law Models and Wave-Optics Codes Over Diverse Low Altitude Operating Regimes," *Directed Energy Professional Society 9th Annual DE Symposium*, Albuquerque, NM, 30 Oct.–2 Nov. 2006.

[21] Cottrell, K. G., Try, P. D., Hodges, D. B., and Wachtmann, R. F., "Electro-Optical Handbook Volume 1: Weather Support for Precision Guided Munitions," Air Weather Service TR, AWS/TR-79/002, 1979.

Gerard Parr
Associate Editor